

Routing Algorithms for Delay-insensitive and Delay-sensitive Applications in Underwater Sensor Networks

Dario Pompili, Tommaso Melodia, Ian F. Akyildiz

Broadband and Wireless Networking Laboratory
School of Electrical & Computer Engineering
Georgia Institute of Technology, Atlanta, GA 30332
{dario, tommaso, ian}@ece.gatech.edu

ABSTRACT

Underwater sensor networks consist of sensors and vehicles deployed to perform collaborative monitoring tasks over a given region. Underwater sensor networks will find applications in oceanographic data collection, pollution monitoring, offshore exploration, disaster prevention, assisted navigation, tactical surveillance, and mine reconnaissance. Underwater acoustic networking is the enabling technology for these applications. In this paper, an architecture for three-dimensional underwater sensor networks is considered, and a model characterizing the acoustic channel utilization efficiency is introduced, which allows investigating some fundamental characteristics of the underwater environment. In particular, the model allows setting the optimal packet size for underwater communications given monitored volume, density of the sensor network, and application requirements. Moreover, the problem of data gathering is investigated at the network layer by considering the cross-layer interactions between the routing functions and the characteristics of the underwater acoustic channel. Two distributed routing algorithms are introduced for delay-insensitive and delay-sensitive applications. The proposed solutions allow each node to select its next hop, with the objective of minimizing the energy consumption taking the varying condition of the underwater channel and the different application requirements into account. The proposed routing solutions are shown to achieve the performance targets by means of simulation.

Categories and Subject Descriptors:

C.2.2 [Computer-Communication Networks]: Network Protocols-*routing protocols*

General Terms: Algorithms, Design, Reliability, Performance.

Keywords: Underwater Sensor Networks, Routing Algorithms.

1. INTRODUCTION

Underwater sensor networks are envisioned to enable applications for oceanographic data collection, ocean sampling, pollution

and environmental monitoring, offshore exploration, disaster prevention, assisted navigation, distributed tactical surveillance, and mine reconnaissance. Multiple Unmanned or Autonomous Underwater Vehicles (UUVs, AUVs), equipped with underwater sensors, will also find application in exploration of natural undersea resources and gathering of scientific data in collaborative monitoring missions. To make these applications viable, there is a need to enable efficient communications among underwater devices. Wireless underwater acoustic networking is the enabling technology for these applications. Underwater Acoustic Sensor Networks (UW-ASNs) [4] consist of sensors that are deployed to perform collaborative monitoring tasks over a given volume of water. To achieve this objective, sensors must be organized in an autonomous network that self-configures according to the varying characteristics of the ocean environment.

Acoustic communications are the typical physical layer technology in underwater networks. In fact, radio waves propagate through conductive salty water only at extra low frequencies (30 – 300 Hz), which require large antennae and high transmission power. For example, the Berkeley MICA2 Motes, the most popular experimental platform in the sensor networking community, have been reported to achieve a transmission range of 120 cm underwater at 433 MHz by experiments performed at the Robotic Embedded Systems Laboratory (RESL) at the University of Southern California. Optical waves do not suffer from such high attenuation but are affected by scattering. Moreover, transmission of optical signals requires high precision in pointing the narrow laser beams. Thus, links in underwater networks are usually based on *acoustic wireless communications* [24].

Many researchers are currently engaged in developing networking solutions for terrestrial wireless ad hoc and sensor networks. Although there exist many recently developed network protocols for wireless sensor networks, the unique characteristics of the underwater acoustic communication channel, such as limited bandwidth capacity and high propagation delays [21], require very efficient and reliable new data communication protocols. Major challenges in the design of underwater acoustic networks are:

1. Propagation delay is five orders of magnitude higher than in radio frequency (RF) terrestrial channels and variable;
2. The underwater channel is severely impaired, especially due to multipath and fading problems;
3. The available bandwidth is severely limited;
4. High bit error rates and temporary losses of connectivity (shadow zones) can be experienced;

Permission to make digital or hard copies of all or part of this work for personal or classroom use is granted without fee provided that copies are not made or distributed for profit or commercial advantage and that copies bear this notice and the full citation on the first page. To copy otherwise, to republish, to post on servers or to redistribute to lists, requires prior specific permission and/or a fee.

MobiCom'06, September 23–26, 2006, Los Angeles, California, USA.
Copyright 2006 ACM 1-59593-286-0/06/0009 ...\$5.00.

5. Underwater sensors are prone to failures because of fouling and corrosion;
6. Battery power is limited and usually batteries cannot be easily recharged, also because solar energy cannot be exploited.

Most impairments of the underwater acoustic channel are adequately addressed at the physical layer, by designing receivers able to deal with high bit error rates, fading, and the inter-symbol interference (ISI) caused by multipath. Conversely, characteristics such as the extremely long and variable propagation delays are better addressed at higher layers. For example, the delay variance in horizontal acoustic links is generally larger than in vertical links due to multipath [24]. In fact, the quality of acoustic links is highly unpredictable, since it mainly depends on fading and multipath, which are not easily modeled phenomena. Finally, as in terrestrial sensor networks, energy conservation is one of the major concerns, since batteries cannot be easily recharged or replaced. Moreover, the bandwidth of the underwater links is severely limited. Hence, routing protocols designed for underwater acoustic networks must be extremely bandwidth and energy efficient.

For these reasons, we introduce a model that allows investigating some fundamental characteristics of the underwater environment. More specifically, the model highlights the underwater acoustic channel utilization efficiency as a function of the distance between the corresponding nodes and of the packet size, by describing the trade-off between the channel efficiency and the packet error rate, both increasing with increasing packet size. The model also allows setting the optimal packet size for underwater communications when a particular forward error correction (FEC) scheme is adopted, given the 3D volume of water that the application needs to monitor, the density of the sensor network, and the application requirements.

Based on the insights provided by the model, we propose new geographical routing algorithms for the 3D underwater environment, designed to distributively meet the requirements of delay-insensitive and delay-sensitive sensor network applications, respectively. The proposed distributed routing solutions are tailored for the characteristics of the underwater environment, e.g., our solutions take explicitly into account the very high propagation delay, which may vary in horizontal and vertical links, the different components of the transmission loss, the impairment of the physical channel, the extremely limited bandwidth, the high bit error rate, and the limited battery energy.

In particular, our routing solutions allow achieving two apparently conflicting objectives, i.e., increasing the efficiency of the channel by transmitting a *train* of short packets *back-to-back*; and limiting the packet error rate by keeping the transmitted packets short. The packet-train concept is exploited in the routing algorithms proposed in this paper. The algorithms are distributed solutions for delay-insensitive and delay-sensitive applications, respectively, and allow each node to *jointly* select its best next hop, the transmitted power, and the forward error correction (FEC) rate for each packet, with the objective of minimizing the energy consumption, taking the condition of the underwater channel and the application requirements into account.

The first algorithm deals with delay-insensitive applications, and tries to exploit links that guarantee a low packet error rate, to maximize the probability that a packet is correctly decoded at the receiver, and thus minimize the number of required packet retransmissions.

The second algorithm is designed for delay-sensitive applications. The objective is to minimize the energy consumption, while statistically limiting the end-to-end packet delay and packet error

rate by estimating at each hop the time to reach the sink and by leveraging statistical properties of underwater links. In order to meet these application-dependent requirements, each node *jointly* selects its best next hop, the transmitted power, and the forward error correction rate for each packet. Differently from the previous delay-insensitive routing solution, next hops are selected by also considering maximum per-packet allowed delay, while unacknowledged packets are not retransmitted to limit the delay.

The emphasis on energy consumption is justified by the need for extended lifetime deployments of underwater sensor networks. While survivability is another fundamental aspect of sensor networks, this has been dealt with in [19], where a two-phase resilient routing algorithm for long-term applications in UW-ASNs is proposed.

The remainder of this paper is organized as follows. In Section 2, we discuss the suitability of the existing ad hoc and sensor routing solutions for the underwater environment, and motivate the use of geographical routing in this environment. In Section 3, we consider a communication architecture for 3D underwater acoustic sensor networks, and introduce the network and propagation models that are used in the routing problem formulations. In Section 4, we discuss the underwater channel utilization efficiency, compare it with the terrestrial radio channel, analyze the packet-train concept to improve the channel efficiency, and cast the optimal packet problem for underwater communications when a particular FEC scheme is adopted, given the application requirements. In Section 5, we introduce a distributed routing algorithm for delay-insensitive applications, while in Section 6 we adapt it to statistically meet the end-to-end delay-sensitive application requirements. Finally, in Section 7 we show the performance results of the proposed solutions, while in Section 8 we draw the main conclusions.

2. RELATED WORK

There has been an intensive study in routing protocols for terrestrial ad hoc [2] and wireless sensor networks [3] in the last few years. However, due to the different nature of the underwater environment and applications, there are several drawbacks with respect to the suitability of the existing terrestrial routing solutions for underwater networks. The existing routing protocols are usually divided into three categories, namely *proactive*, *reactive*, and *geographical* routing protocols.

Proactive protocols (e.g., DSDV [18], OLSR [10]) provoke a large signaling overhead to establish routes for the first time and each time the network topology is modified because of mobility or node failures, since updated topology information has to be propagated to all network devices. This way, each device is able to establish a path to any other node in the network, which may not be needed in UW-ASNs. For this reason, proactive protocols are not suitable for underwater networks.

Reactive protocols (e.g., AODV [17], DSR [11]) are more appropriate for dynamic environments but incur a higher latency and still require source-initiated flooding of control packets to establish paths. Reactive protocols are unsuitable for UW-ASNs as they also cause a high latency in the establishment of paths, which is even amplified underwater by the slow propagation of acoustic signals. Moreover, the topology of UW-ASNs is unlikely to vary dynamically on a short-time scale.

Geographical routing protocols (e.g., GFG [6], PTKF [14]) are very promising for their scalability feature and limited required signaling. However, GPS (Global Positioning System) radio receivers, which may be used in terrestrial systems to accurately estimate the geographical location of sensor nodes, do not work properly in the underwater environment. In fact, GPS uses waves in the 1.5 GHz

band and those waves do not propagate in water. Still, underwater devices (sensors, UUVs, UAVs, etc.) need to estimate their current position, irrespective of the chosen routing approach. In fact, it is necessary to associate the sampled data with the 3D position of the device that generates the data, to spatially reconstruct the characteristics of the event. Underwater localization can be achieved by leveraging the low speed of sound in water, which permits accurate timing of signals, and pairwise node distance data can be used to perform 3D localization, similar to the 2D localization demonstrated in [16]. However, low-complexity acoustic techniques to solve the underwater localization problem with limited energy expenditure in the presence of measurement errors need to be further investigated by the research community.

Some recent papers propose network layer protocols specifically tailored for underwater acoustic networks. In [29], a routing protocol is proposed that autonomously establishes the underwater network topology, controls network resources, and establishes network flows, which relies on a centralized network manager running on a surface station. The manager establishes efficient data delivery paths in a centralized fashion, which allows avoiding congestion and providing some form of quality of service guarantee. Although the idea is promising, the performance evaluation of the proposed mechanisms has not been thoroughly studied.

In [19], the problem of data gathering for three-dimensional underwater sensor networks is investigated at the network layer by considering the interactions between the routing functions and the characteristics of the underwater acoustic channel. A two-phase resilient routing solution for long-term monitoring missions is developed, with the objective of guaranteeing survivability of the network to node and link failures. In the first phase energy-efficient node-disjoint primary and backup paths are optimally configured, by relying on topology information gathered by a surface station, while in the second phase paths are locally repaired in case of node failures.

In [30], a vector-based forwarding routing is developed, which does not require state information on the sensors and only involves a small fraction of the nodes in routing. The proposed algorithm, however, does not consider applications with different requirements.

In [23], the authors provide a simple design example of a shallow water network, where routes are established by a central manager based on neighborhood information gathered from all nodes by means of poll packets. However, the paper does not describe routing issues in detail, e.g., it does not discuss the criteria used to select data paths. Moreover, sensors are only deployed linearly along a stretch, while the characteristics of the 3D underwater environment are not investigated.

In [28], a long-term monitoring platform for underwater sensor networks consisting of static and mobile nodes is proposed, and hardware and software architectures are described. The nodes communicate point-to-point using a high-speed optical communication system, and broadcast using an acoustic protocol. The mobile nodes can locate and hover above the static nodes for data muling, and can perform useful network maintenance functions such as deployment, relocation, and recovery. However, due to the limitations of optical transmissions, communication is enabled only when the sensors and the mobile mules are in close proximity.

A few experimental implementations of underwater acoustic sensor networks have been reported in the last few years. The Front-Resolving Observational Network with Telemetry project relies on acoustic telemetry and ranging advances pursued by the US Navy referred to as “telesonar” technology [7]. The Seaweb network for FRONT Oceanographic Sensors involves telesonar modems deployed in conjunction with sensors, gateways, and repeaters, to en-

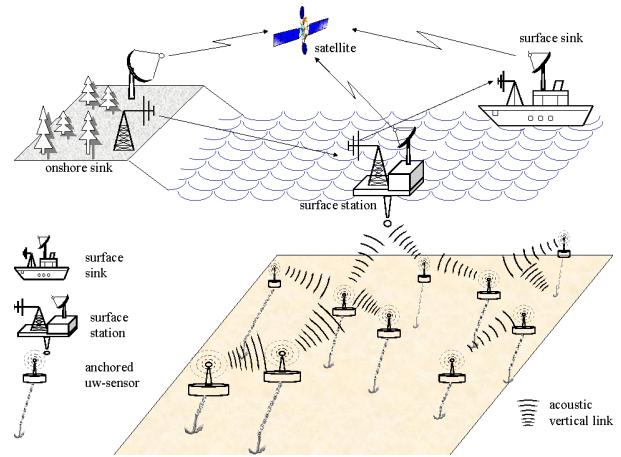


Figure 1: Architecture for 3D Underwater Sensor Networks

able sensor-to-shore data delivery and shore-to-sensor remote control. Researchers from different fields gathered at the Monterey Bay Aquarium Research Institute in August 2003 and July 2006 to quantify gains in predictive skills for principal circulation trajectories, i.e., to study upwelling of cold, nutrient-rich water in the Monterey Bay, and to analyze how animals adapt to life in the deep sea.

3. NETWORK ARCHITECTURE

In this section, we consider a communication architecture for three-dimensional underwater sensor networks and the network and propagation models that will be used in the formulation of our routing algorithms. These networks are used to detect and observe phenomena that cannot be adequately observed by means of ocean bottom sensor nodes, i.e., to perform cooperative sampling of the 3D ocean environment. In three-dimensional underwater networks, uw-sensor nodes float at *different depths* to observe a given phenomenon. One possible solution would be to attach each sensor node to a surface buoy, by means of wires whose length can be regulated to adjust the depth of each sensor node. However, although this solution enables easy and quick deployment of the sensor network, multiple floating buoys may obstruct ships navigating on the surface, or they can be easily detected and deactivated by enemies in military settings. Furthermore, floating buoys are vulnerable to weather and tampering or pilfering.

A different approach is to anchor winch-based sensor devices to the bottom of the ocean, as depicted in Fig. 1. Each sensor is equipped with a floating buoy that can be inflated by a pump. The buoy pulls the sensor towards the ocean surface. The depth of the sensor can then be regulated by adjusting the length of the wire that connects the sensor to the anchor, by means of an electronically controlled engine that resides on the sensor. Sensor should coordinate their depths in such a way as to guarantee that the network topology be always connected, i.e., at least one path from every sensor to the surface station always exists, and achieve communication coverage [22], as further discussed in [4]. Although AUVs can add a remarkable degree of flexibility to the network architecture, they also introduce new important challenges due to their mobility. Hence, the study of the impact of mobility on underwater routing is left for future work.

3.1 Network Model

The underwater network can be represented as a graph $\mathcal{G}(\mathcal{V}, \mathcal{E})$, where $\mathcal{V} = \{v_1, \dots, v_N\}$ is a finite set of nodes in a finite-dimension 3D volume, with $N = |\mathcal{V}|$, and \mathcal{E} is the set of links among nodes, i.e., e_{ij} equals 1 if nodes v_i and v_j are within each other's transmission range. Node v_N (also N for simplicity) represents the sink, i.e., the surface station. Each link e_{ij} is associated with its mean propagation delay \overline{T}_{ij}^q and with the standard deviation of the propagation delay, σ_{ij}^q . All these values are dependent on the 3D positions of nodes v_i and v_j (also i and j for simplicity in the following). \mathcal{S} is the set of sources, which includes those sensors that sense information from the underwater environment and send it to the surface station N .

3.2 Underwater Propagation Model

The underwater transmission loss describes how the acoustic intensity decreases as an acoustic pressure wave propagates outwards from a sound source. The transmission loss $TL(d, f)$ [dB] that a narrow-band acoustic signal centered at frequency f [KHz] experiences along a distance d [m] can be described by the Urick propagation model [27],

$$TL(d, f) = \chi \cdot \text{Log}(d) + \alpha(f) \cdot d + A. \quad (1)$$

In (1), the first term account for *geometric spreading*, which refers to the spreading of sound energy as a result of the expansion of the wavefronts. It increases with the propagation distance and is independent of frequency. There are two common kinds of geometric spreading: *spherical* (omni-directional point source, spreading coefficient $\chi = 20$), which characterizes deep water communications, and *cylindrical* (horizontal radiation only, spreading coefficient $\chi = 10$), which characterizes shallow water communications. In-between cases show a spreading coefficient χ in the interval (10, 20), depending on water depth and link length. The second term accounts for *medium absorption*, where $\alpha(f)$ [dB/m] represents an absorption coefficient that describes the dependency of the transmission loss on the frequency band, as shown in Fig. 2. Finally, the last term, expressed by the quantity A [dB], is the so-called *transmission anomaly*, and accounts for the degradation of the acoustic intensity caused by multiple path propagation, refraction, diffraction, and scattering of sound caused by particulates, bubbles, and plankton within the water column. Its value is higher for shallow-water horizontal links (up to 10 dB), which are more affected by multipath [27]. More details can be found in [8] and [12].

In [27], the underwater acoustic propagation speed $q(z, S, t)$ [m/s] is also accurately modeled as

$$q(z, S, t) = 1449.05 + 45.7 \cdot t - 5.21 \cdot t^2 + 0.23 \cdot t^3 + (1.333 - 0.126 \cdot t + 0.009 \cdot t^2) \cdot (S - 35) + 16.3 \cdot z + 0.18 \cdot z^2, \quad (2)$$

where $t = T/10$ (T is the temperature in $^{\circ}\text{C}$), S is the salinity in *ppt*, and z is the depth in km. The above expression provides a useful tool to determine the propagation speed, and thus the propagation delay, in different operating conditions, and yields values in [1460, 1520] m/s, centered around 1500 m/s.

4. UNDERWATER CHANNEL EFFICIENCY AND OPTIMAL PACKET SIZE

In this section, we introduce an analytical model to study the effect of the characteristics of the underwater environment on the channel utilization efficiency, in order to provide guidelines for the design of routing solutions. In particular, in Section 4.1 we analyze

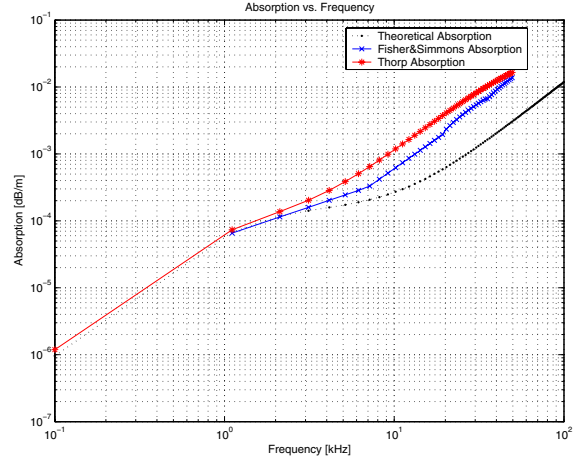


Figure 2: Theoretical, Fisher&Simon’s, and Thorp’s medium absorption coefficient $\alpha(f)$ vs. frequency $f \in [10^{-1}, 10^2]$ KHz

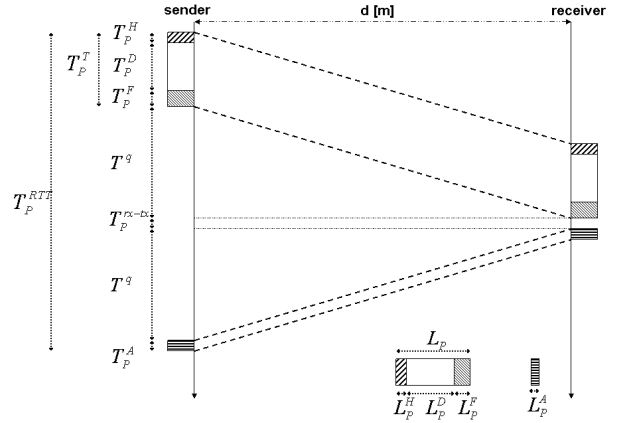


Figure 3: Single-packet transmission scheme

the *single-packet* transmission scheme, while in Section 4.2 we propose the *packet-train* scheme to enhance the channel efficiency and derive the optimal packet size. While the optimal packet size at the data link layer in an underwater channel has been analytically derived in [25], our analysis accounts for cross-layer interactions with medium access control (MAC) layers and forward error correction schemes, which cannot be neglected in the harsh underwater environment. The packet optimization analysis in [25], in fact, does not consider the extra-overhead caused by the adopted FEC scheme, nor does it evaluate the number of required packet retransmissions, which depends on the experienced packet error rate (PER), and ultimately on the state of the underwater channel.

4.1 Single-packet Transmission Scheme

We consider a shared channel where a device transmits a data packet when it senses the channel idle, and the corresponding device advertises a correct reception with a short acknowledge (ACK) packet. By referring to Fig. 3, we assume that the payload of the data packet to be transmitted has size L_p^D bits, while the header has size L_p^H bits. Moreover, the packet may be protected with a FEC mechanism, which introduces a redundancy of L_p^F bits. The ACK

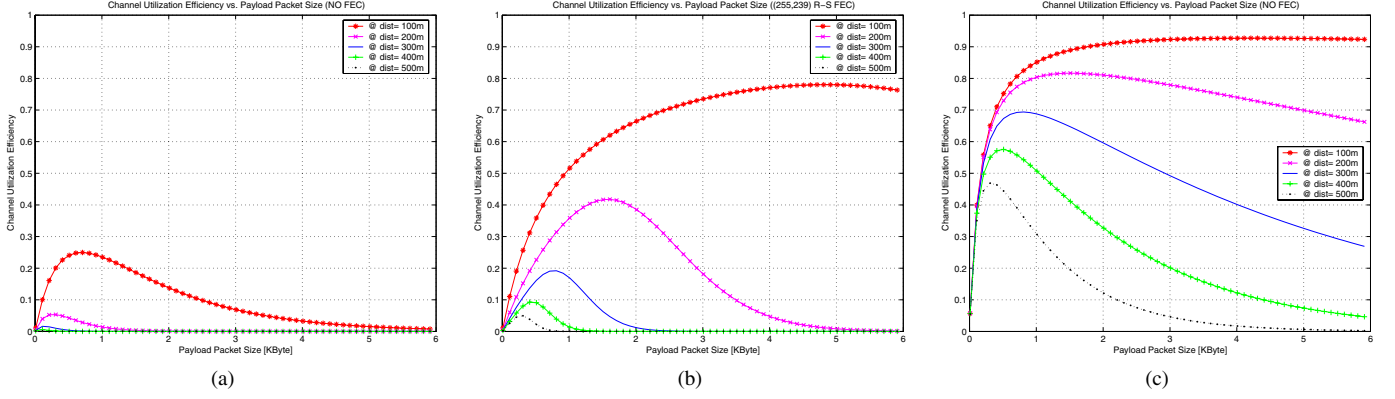


Figure 4: Underwater and terrestrial channel utilization efficiency for different distances (100 m – 500 m). (a): Underwater channel efficiency vs. packet payload size without FEC; (b): Underwater channel efficiency vs. packet payload size with (255, 239) Reed-Solomon FEC; (c): Terrestrial channel efficiency vs. packet payload size without FEC

packet is assumed to be L_P^A bits long. Given a transmission rate r , the *packet round-trip time* T_P^{RTT} is

$$T_P^{RTT} = T_P^H + T_P^D + T_P^F + 2 \cdot T^q + T_P^{rx-tx} + T_P^A, \quad (3)$$

where T_P^H , T_P^D , T_P^F , and T_P^A are the transmission times of the header, payload, FEC overhead, and ACK packet, respectively, while T^q is the propagation delay, and T_P^{rx-tx} is the time needed to process the packet and switch the circuitry from receiving to transmitting mode. We define the *channel utilization efficiency* η as

$$\eta = \frac{1}{r} \cdot \frac{L_P^D}{\hat{N}^{TX} \cdot T_P^{RTT}}, \quad (4)$$

where \hat{N}^{TX} represents the average number of transmissions needed for the packet to be successfully decoded at the receiver, i.e.,

$$\hat{N}^{TX} = \frac{1}{1 - \psi^{\mathcal{F}}(L_P, L_P^F, BER)}, \quad (5)$$

where $\psi^{\mathcal{F}}()$ represents the *packet error rate* (PER) given the packet size L_P and the *bit error rate* (BER) on the link, when a FEC scheme \mathcal{F} with redundancy L_P^F is adopted. Equation (5) assumes independent errors among adjacent packets, which holds when the channel coherence time is shorter than the average retransmission delay, i.e., the average time that a sender needs to retransmit an unacknowledged packet. We refer to the expression $r \cdot \eta = L_P^D / (\hat{N}^{TX} \cdot T_P^{RTT})$ in (4) as *effective link capacity* between the sender and the receiver; it represents the average bit rate achievable by a contention-free medium access control protocol when a single-packet transmission scheme is adopted.

By substituting (3) into (4), we obtain

$$\eta = \frac{L_P^D}{\hat{N}^{TX} \cdot [L_P^D + L_P^H + L_P^F + L_P^A + r \cdot (2\frac{d}{q} + T_P^{rx-tx})]}, \quad (6)$$

where the propagation delay T^q is expressed as the ratio between the distance d between the sender and the receiver, and the speed q of the signal in the medium, expressed in (2).

Figures 4(a) and 4(b) show the channel efficiency (6) for an underwater environment, where we set the speed of sound in water to $q = 1500$ m/s (see Section 3.2), and the transmission rate to $r = 50$ Kbps [24]. In particular, Fig. 4(a) refers to transmissions without forward error correction (i.e., $L_P^F = 0$), while Fig. 4(b) refers to a (255, 239) Reed-Solomon (R-S) FEC [20]. Although

a thorough study of the performance of different FEC schemes in the underwater environment is out of the scope of this paper, we chose Reed-Solomon FEC since large block codes are easy to generate and provide excellent burst-error detection and correcting ability. Note that R-S codes are widely used in conjunction with Viterbi-decoded convolutional codes to correct the errors made by the Viterbi decoder. In fact, because of the nonlinear nature of Viterbi decoding, these errors occur in bursts even when channel errors are random, as with Gaussian noise. The bit error rate on the channel is assumed to be linearly increasing with decreasing signal-to-noise ratio (SNR), for the sake of simplicity. In particular, the BER is assumed to range in the interval $[10^{-2}, 10^{-6}]$, as indicated in [23]. In addition, errors are assumed to be uniformly distributed in time. The two figures consider a range of distances between 100 m and 500 m. As can be seen in Fig. 4(a), the maximum channel efficiency is 0.25 over a distance of 100 m with packet payload size equal to about 0.8 KByte, while it drops below 0.05 for distances greater than 200 m. When we apply a (255, 239) R-S FEC technique in the same environment, a maximum channel utilization efficiency of 0.77 can be achieved over 100 m with packet payloads of 5 KByte. The efficiency degrades abruptly with increasing distance, and the optimal packet size, i.e., the packet size that yields maximum channel efficiency on a given distance, decreases as well. Larger packets tend to improve the channel efficiency; at the same time, given a bit error rate, the packet error rate increases with increasing packet size, thus increasing the average number of transmissions for a single packet. Hence, the optimal packet size is determined as the equilibrium between these two contrasting phenomena.

Figure 4(c) shows the same phenomena for a terrestrial radio channel, where we set the propagation speed q to $3 \cdot 10^8$ m/s and the transmission rate r to 1 Mbps. The bit error rate on the channel is assumed to be linearly increasing with decreasing SNR (between 10^{-3} and 10^{-7}). With respect to the underwater environment, the channel efficiency values are higher and degrade more smoothly with increasing distance. In general, the optimal packet sizes in this environment are smaller with respect to the underwater case. If we then protect a packet with FEC techniques, we obtain very high efficiencies (in the order of 0.9 – 0.95) for a wide range of distances and packet sizes.

To summarize, we observe the following facts when a single-packet transmission scheme in the underwater environment is used:

1. The channel efficiency is very low. This, combined with very low data rates, may be detrimental for communications. Hence, it is crucial to maximize the efficiency in exploiting the available resources.
2. Underwater communications greatly benefit from the use of forward error correction (FEC) and hybrid automatic request (ARQ) mechanisms. In fact, combined FEC and ARQ strategies can consistently decrease the average number of transmissions. The increasing packet error rate on longer-range underwater links can be compensated for by either decreasing the packet length, or by applying stronger FEC/ARQ algorithms. As we have shown, in the underwater environment the optimal packet size is considerably affected by the use of FEC techniques; this explains why, differently from [25], we incorporated the effect of FEC schemes in the optimization problem.
3. The channel efficiency drops abruptly with increasing distance, and with varying packet size. In particular, i) the average number of packet retransmissions increases as the packet size increases, ii) the efficiency decreases as the number of retransmissions increases, and iii) the efficiency increases as the packet payload size increases. Consequently, the optimal packet size should be determined by considering the trade-off between channel efficiency and retransmissions.

4.2 Packet Train and Optimal Packet Size

To overcome the problems raised by the single-packet transmission scheme, which ultimately leads to low channel efficiencies, we exploit the concept of *packet train*. As shown in Fig. 5(a), a packet train is a *juxtaposition* of packets, which are transmitted *back-to-back* by a node without releasing the channel, in a *single atomic transmission*. For delay-insensitive applications, the corresponding node sends for each train an ACK, which can either *cumulatively acknowledge* the whole train, i.e., all the consecutively transmitted packets, or it can *selectively* request the retransmission of specific packets (which are then included in the next train). In general, a selective repeat approach is to be preferred.

In Section 4.1, we discussed the existing trade-off between the channel efficiency and the packet error rate, both increasing with increasing packet size. The strategy proposed here allows increasing the efficiency of the channel by increasing the length of the transmitted train, without compromising on the packet error rate, i.e., keeping the transmitted packets short. In other words, we *decouple* the effect of the packet size from the choice of the length of the train, i.e., the number of consecutive packets transmitted back-to-back by a node: while the former determines the packet error rate, the latter can be increased as needed to increase the channel efficiency. Thus, the channel efficiency associated with the packet-train scheme can be computed as

$$\eta = \eta_T(L_T) \cdot \eta_P(L_P, L_P^F), \quad (7)$$

where $\eta_T(L_T)$ is the packet-train efficiency, i.e., the ratio between the train payload transmission time and the *train round-trip time* T_T^{RTT} (see Fig. 5(a)) normalized to the bit rate r ,

$$\eta_T(L_T) = \frac{L_T^D}{L_T^D + L_T^H + L_T^A + r \cdot (2\frac{d}{q} + T_T^{rx-tx})}, \quad (8)$$

whose expression is similar to (6), and $\eta_P(L_P, L_P^F)$ is the packet efficiency, i.e., the ratio of the packet payload and the packet size multiplied by the average number of transmissions such that a packet

is successfully decoded at the receiver, formally defined as

$$\eta_P(L_P, L_P^F) = \frac{L_P - L_P^H - L_P^F}{\hat{N}^{TX} \cdot L_P}. \quad (9)$$

Equation (7) accounts for the decoupling between train length, which solely affects the train efficiency η_T , and choice of the packet structure, which solely affects the packet efficiency η_P .

The optimal packet size (L_P^*) and optimal FEC redundancy (L_P^{F*}) are chosen in such a way as to maximize the packet efficiency η_P , as cast in the optimal packet size problem.

$\mathbf{P_P^{size}}$: Optimal Packet Size Problem in UW-ASNs

Given : $L_P^H, \bar{P}_{max}^{TX}, r, f_0, \bar{N}_0, \text{Pr}\{l\}, \psi^{\mathcal{F}}, \Phi^{\mathcal{M}}, PER_{max}^{e2e}$
Find : L_P^*, L_P^{F*}
Maximize : $\eta_P(L_P, L_P^F) = \frac{L_P - L_P^H - L_P^F}{\hat{N}^{TX} \cdot L_P}$
Subject to :

$$BER = \Phi^{\mathcal{M}}\left(\frac{\bar{P}_{max}^{TX}}{r \cdot \bar{N}_0 \cdot \overline{TL}}\right); \overline{TL} = \int_0^\infty TL(l, f_0) \cdot \text{Pr}\{l\} dl; \quad (10)$$

(Delay – insensitive Applications)

$$\hat{N}^{TX} = \frac{1}{1 - \psi^{\mathcal{F}}(L_P, L_P^F, BER)}; \quad (11)$$

(Delay – sensitive Applications)

$$\hat{N}^{TX} = 1; \quad (12)$$

$$1 - \left[1 - \psi^{\mathcal{F}}(L_P, L_P^F, BER)\right]^{N_{max}^{Hop}} \leq PER_{max}^{e2e}. \quad (13)$$

Where:

- $P_{i,max}^{TX}$ [W] is the maximum transmitting power for node i , and \bar{P}_{max}^{TX} [W] is the average among all nodes of the maximum transmitting power.
- $TL(l, f_0)$ [dB] is the transmission loss at distance l and frequency f_0 , as described in Section 3.2, while r [bps] is the considered bit rate.
- $\text{Pr}\{l\}$ is the distance distribution between neighboring nodes, which depends on how nodes are statistically deployed in the volume; for a random 3D deployment, $\text{Pr}\{l\}$ is derived in [15].
- \hat{N}^{TX} is the estimated number of transmissions of a packet such that it is correctly decoded at the receiver.
- $\Phi^{\mathcal{M}}\left(\frac{\bar{P}_{max}^{TX}}{r \cdot \bar{N}_0 \cdot \overline{TL}}\right)$ represents the average bit error rate (BER) on a link; it is a function of the ratio between the average energy of the received bit $\bar{P}_{max}^{TX}/(r \cdot \overline{TL})$ and the expected noise \bar{N}_0 at the receiver, and it depends on the modulation scheme \mathcal{M} ; in general, the noise has a thermal, an ambient, and a man-made component; several studies of shallow water noise measurements [9] suggest considering an average value of 70 dB $_{\mu\text{Pa}}$ for the ambient noise.
- $PER = \psi^{\mathcal{F}}(L_P, L_P^F, BER)$ represents the packet error rate, given the packet size L_P , the FEC redundancy L_P^F , and the bit error rate (BER), and it depends on the adopted FEC technique \mathcal{F} .

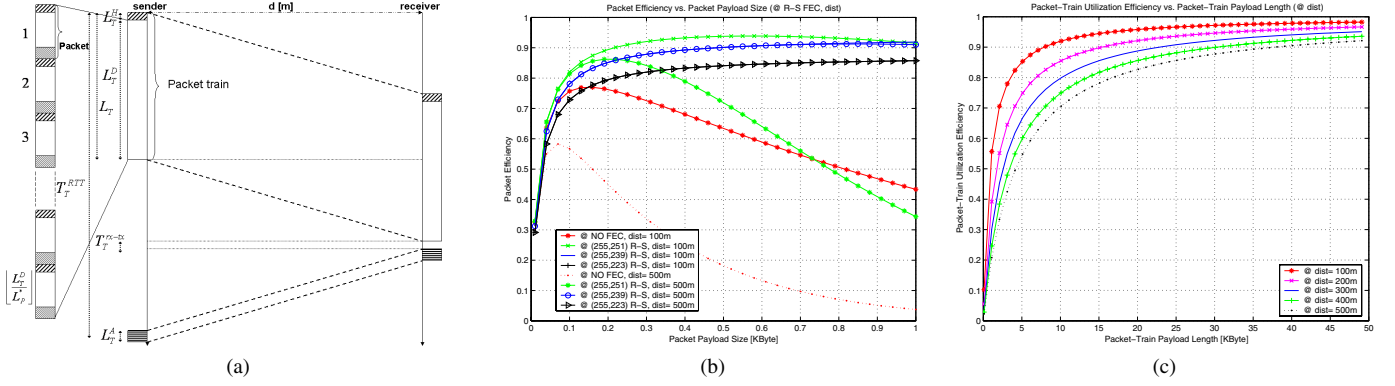


Figure 5: Packet-train performance. (a): Packet-train transmission scheme; (b): Underwater packet efficiency vs. packet payload size for different distances (100 m and 500 m); (c): Packet-train efficiency vs. packet-train payload length for different distances (100 m-500 m)

- PER_{max}^{e2e} is the application maximum allowed end-to-end packet error rate, while N_{max}^{Hop} is the maximum expected number of hops, function of the network diameter [22].

The optimum packet size L_P^* is found by maximizing the packet efficiency η_P (9) for different FEC schemes \mathcal{F} and code rates L_P^F , under proper sets of constraints for delay-insensitive [(10),(11)] and -sensitive [(10),(12),(13)] applications. The packet size is optimized given the distance distribution between neighboring nodes ($\Pr\{l\}$), which determines the average transmission loss \overline{TL} (see Section 3.2), and ultimately the BER, computed as a function $\Phi^{\mathcal{M}}()$ of the modulation scheme \mathcal{M} and the average signal-to-noise ratio at the receiver, as formally defined in (10). Thus, $\mathbf{P}_P^{\text{size}}$ finds the optimal packet size and packet FEC redundancy, given the device characteristics ($\overline{P}_{max}^{TX}, r, f_0, \psi^{\mathcal{F}}, \Phi^{\mathcal{M}}$), the deployment volume and node density, which impact the distribution between neighboring nodes ($\Pr\{l\}$), and the average ambient noise (\overline{N}_0), as

$$(L_P^*, L_P^{F*}) = \underset{(L_P, L_P^F)}{\operatorname{argmax}} \eta_P(L_P, L_P^F). \quad (14)$$

Figure 5(b) shows the underwater packet efficiency η_P when the packet payload size L_P^D varies, for different distances (100 m and 500 m). In particular, for a volume with an average node distance of 100 m, the highest packet efficiency ($\eta_P^* = 0.94$) is achieved with a packet payload size of $L_P^{D*} = 0.55$ KByte and a (255, 251) R-S FEC, while for a volume with an average node distance of 500 m, the highest packet efficiency ($\eta_P^* = 0.91$) is achieved with a packet payload size of $L_P^{D*} = 0.9$ KByte and a (255, 239) R-S FEC.

Figure 5(c) depicts the train efficiency η_T when the train payload length L_T^D varies, for different distances (100 m-500 m). Since the train efficiency monotonically increases as the train payload length increases for every distance, we can increase the train efficiency as needed with the only constraints being that: i) sensor buffer size is limited, and ii) short-term fairness among sensors competing to access the medium decreases as the train payload length increases.

To summarize, $\mathbf{P}_P^{\text{size}}$ finds *off-line* the optimal packet size and packet FEC redundancy for delay-insensitive and -sensitive applications, whereas the distributed algorithms proposed in the following sections adjust *on-line* the strength of the FEC technique by tuning the amount of FEC redundancy according to the dynamic channel conditions, given the *fixed* packet size L_P^* . The choice of a fixed packet size for UW-ASNs is motivated by the need for system simplicity and ease of sensor buffer management. In fact, a

design proposing per-hop optimal packet size, e.g., solving $\mathbf{P}_P^{\text{size}}$ for any link distance and use the resulting *distance-dependent* optimal packet size in the routing algorithms, would encounter several implementation problems, such as the need of segmentation and re-assembled functionalities that incur in tremendous overhead, which is unlikely affordable by the low-end sensor nodes.

Throughout this section, we referred to a simple CSMA-like MAC, where a device transmits a data packet when it senses the shared channel idle, and the corresponding device advertises correct reception with a short ACK packet. Although we do not advocate this access scheme for this environment, the results of our analysis are valid when a modified version of the widely used 802.11 MAC is adopted for UW-ASNs. Moreover, the results about the channel efficiency motivate the need for the development of a new multiple access technique for the underwater environment. To this end, we are currently developing a distributed CDMA-based MAC tailored for the underwater environment.

5. ROUTING ALGORITHM FOR DELAY-INSENSITIVE APPLICATIONS

In this section, we introduce a distributed geographical routing solution for delay-insensitive underwater applications. Most of prior research in geographical routing protocols assumes that nodes can either work in a *greedy mode* or in a *recovery mode*. When in greedy mode, the node that currently holds the message tries to forward it towards the destination. The recovery mode is entered when a node fails to forward a message in the greedy mode, since none of its neighbors is a feasible next hop. Usually this occurs when the node observes a void region between itself and the destination. Such a node is referred to as *concave* node. For example, the GPSR algorithm [13] makes greedy forwarding decisions. When a packet reaches a concave node, GPSR tries to recover by routing around the perimeter of the void region. Recovery mechanisms, which allow a packet to be forwarded to the destination when a concave node is reached, are out of the scope of this paper. For this reason, the protocol proposed in this section assumes that no void regions exist, although it can be enhanced by combining it with one of the existing recovery mechanisms (e.g., [6]).

The objective of our proposed solution is to efficiently exploit the channel, as discussed in Section 4, and to minimize the energy consumption. The proposed algorithm relies on the packet-train transmission scheme, presented in Section 4.2. In a distributed fashion,

it allows each node to *jointly* select its best next hop, the transmitted power, and the FEC code rate for each packet, with the objective of minimizing the energy consumption, taking the condition of the underwater channel into account. Furthermore, it tries to exploit those links that guarantee a low packet error rate, in order to maximize the probability that the packet is correctly decoded at the receiver. For these reasons, the energy efficiency of the link is weighted with the number of retransmissions required to achieve link reliability, with the objective of saving energy. We can now cast the delay-insensitive distributed routing problem.

$\mathbf{P}_{\text{insen}}^{\text{dist}}$: Delay-insensitive Distributed Routing Problem

Given : $i, \mathcal{S}_i, \mathcal{P}_i^N, L_P^*, L_P^H, E_{elec}^b, r, \hat{N}_{0j}, P_{i,max}^{TX}$

Find : $j^* \in \mathcal{S}_i \cap \mathcal{P}_i^N, P_{ij^*}^{TX*} \leq P_{i,max}^{TX}$

$$\text{Minimize : } E_i^{(j)} = E_{ij}^b \cdot \frac{L_P^*}{L_P^* - L_P^H - L_{P_{ij}}^F} \cdot \hat{N}_{ij}^{TX} \cdot \hat{N}_{ij}^{Hop} \quad (15)$$

Subject to :

$$E_{ij}^b = 2 \cdot E_{elec}^b + \frac{P_{ij}^{TX}}{r}; \quad (16)$$

$$L_{P_{ij}}^F = \Psi^{\mathcal{F}^{-1}} \left(L_P^*, PER_{ij}, \Phi^{\mathcal{M}} \left(\frac{P_{ij}^{TX}}{\hat{N}_{0j} \cdot r \cdot TL_{ij}} \right) \right); \quad (17)$$

$$\hat{N}_{ij}^{TX} = \frac{1}{1 - PER_{ij}}; \hat{N}_{ij}^{Hop} = \max \left(\frac{d_{iN}}{\langle d_{ij} \rangle_{> iN}}, 1 \right). \quad (18)$$

Where:

- $L_P^* = L_P^H + L_{P_{ij}}^F + L_{P_{ij}}^N$ [bit] is the *fixed* optimal packet size, solution of $\mathbf{P}_P^{\text{size}}$ (see Section 4.2), where L_P^H is the *fixed* header size of a packet, while $L_{P_{ij}}^F$ is the *variable* FEC redundancy that is included in each packet transmitted from node i to j ; thus, $L_{P_{ij}}^N = L_P^* - L_P^H - L_{P_{ij}}^F$ is the *variable* payload size of each packet transmitted in a train on link (i, j) .
- $E_{elec}^b = E_{elec}^{\text{trans}} = E_{elec}^{\text{rec}}$ [J/bit] is the *distance-independent* energy to transit one bit, where E_{elec}^{trans} is the energy per bit needed by transmitter electronics (PLLs, VCOs, bias currents, etc.) and digital processing, and E_{elec}^{rec} represents the energy per bit utilized by receiver electronics. Note that E_{elec}^{trans} does not represent the overall energy to transmit a bit, but only the distance-independent portion of it.
- $E_{ij}^b = 2 \cdot E_{elec}^b + P_{ij}^{TX}/r$ [J/bit] accounts for the energy to transmit one bit from node i to node j , when the transmitted power and the bit rate are P_{ij}^{TX} [W] and r [bps], respectively. The second term represents the *distance-dependent* portion of the energy necessary to transmit a bit.
- TL_{ij} [dB] is the transmission loss from i to j (see Section 3.2).
- \hat{N}_{ij}^{TX} is the average number of transmissions of a packet sent by node i such that the packet is correctly decoded at receiver j .
- $\hat{N}_{ij}^{Hop} = \max \left(\frac{d_{iN}}{\langle d_{ij} \rangle_{> iN}}, 1 \right)$ is the estimated number of hops from node i to the surface station (sink) N when j is selected as next hop, where d_{ij} is the distance between i and j , and $\langle d_{ij} \rangle_{> iN}$ (which we refer to as *advance*) is the projection of d_{ij} onto the line connecting node i with the sink.

- $BER_{ij} = \phi^{\mathcal{M}}(E_{rec}^b/\hat{N}_{0j})$ represents the bit error rate on link (i, j) ; it is a function of the ratio between the energy of the received bit, $E_{rec}^b = P_{ij}^{TX}/(r \cdot TL_{ij})$, and the expected noise at node j , \hat{N}_{0j} , and it depends on the adopted modulation scheme \mathcal{M} .
- $L_{P_{ij}}^F = \psi^{\mathcal{F}^{-1}}(L_P^*, PER_{ij}, BER_{ij})$ returns the needed FEC redundancy, given the optimal packet size L_P^* , the packet error rate and bit error rate on link (i, j) , and it depends on the adopted FEC technique \mathcal{F} .
- \mathcal{S}_i is the *neighbor set* of node i , while \mathcal{P}_i^N is the *positive advance set*, composed of nodes closer to sink N than node i , i.e., $j \in \mathcal{P}_i^N$ iff $d_{jN} < d_{iN}$.

According to the proposed distributed routing algorithm for delay-insensitive applications, i will select j^* as its best next hop iff

$$j^* = \underset{j \in \mathcal{S}_i \cap \mathcal{P}_i^N}{\text{argmin}} E_i^{(j)*}, \quad (19)$$

where $E_i^{(j)*}$ represents the minimum energy required to successfully transmit a payload bit from node i to the sink, taking the condition of the underwater channel into account, when i selects j as next hop. This link metric, objective function (15) in $\mathbf{P}_{\text{insen}}^{\text{dist}}$, takes into account the number of packet transmissions (\hat{N}_{ij}^{TX}) associated with link (i, j) , given the optimal packet size (L_P^*) and the optimal combination of FEC ($L_{P_{ij}}^F$) and transmitted power (P_{ij}^{TX*}). Moreover, it accounts for the average hop-path length (\hat{N}_{ij}^{Hop}) from node i to the sink when j is selected as next hop, by assuming that the following hops will guarantee the same advance towards the surface station (sink). While this technique to estimate the number of remaining hops towards the surface station is simple, several advantages can be pointed out, as described in [26], such as: i) it does not incur any signaling overhead since it is locally computed and does not require end-to-end information exchange; ii) its accuracy increases as the density increases; iii) its accuracy increases as the distance between the surface station and the current node decreases. For these reasons, we decided to use this method rather than trying to estimate the exact number of hops towards the destination. Simulation performance in Section 7 shows the effectiveness of this choice.

The link metric $E_i^{(j)*}$ in (19) stands for the optimal energy per payload bit when i transmits a packet train to j using the optimal combination of power P_{ij}^{TX*} and FEC redundancy $L_{P_{ij}}^F$ to achieve link reliability, jointly found by solving problem $\mathbf{P}_{\text{insen}}^{\text{dist}}$. This interpretation allows node i to optimally decouple $\mathbf{P}_{\text{insen}}^{\text{dist}}$ into two *sub-problems*: first, minimize the link metric $E_i^{(j)}$ for each of its feasible next-hop neighbors; second, pick as best next hop that node j^* associated with the minimal link metric. This means that the generic node i does not have to solve a complicated optimization problem to find its best route towards a sink. Rather, it needs to sequentially solve the two aforementioned low-complexity sub-problems, each characterized by a complexity $O(|\mathcal{S}_i \cap \mathcal{P}_i^N|)$, i.e., proportional to the number of its neighboring nodes with positive advance towards the sink. Moreover, this operation does not need to be performed each time a sensor has to route a packet, but only when the channel conditions have consistently changed. To summarize, the proposed routing solution allows node i to select as next hop that node j^* among its neighbors that satisfies the following requirements: i) it is closer to the surface station than i , and ii) it minimizes the link metric $E_i^{(j)*}$.

6. ROUTING ALGORITHM FOR DELAY-SENSITIVE APPLICATIONS

Similarly to the delay-insensitive algorithm introduced in Section 5, this algorithm allows each node to distributively select the optimal next hop, the optimal transmitting power, and FEC packet rate, with the objective of minimizing the energy consumption. However, this algorithm includes two new constraints to statistically meet the delay-sensitive application requirements:

1. The end-to-end packet error rate should be lower than an application-dependent threshold PER_{max}^{e2e} ;
2. The probability that the end-to-end packet delay be over a delay bound B_{max} , should be lower than an application-dependent parameter γ .

As a design guideline to meet these requirements, differently from the routing algorithm for delay-insensitive applications, the proposed algorithm does not retransmit corrupted or lost packets at the link layer. Rather, it discards corrupted packets. Moreover, it time-stamps packets when they are generated by a source so that it can discard expired packets. To save energy, while statistically limiting the end-to-end packet delay, we rely on an *earliest deadline first* scheduling, which dynamically assigns higher priority to packets closer to their deadline, as shown in Section 6.1. We can now cast the delay-sensitive distributed routing problem.

\mathbf{P}_{sen}^{dist} : Delay-sensitive Distributed Routing Problem

Given : $i, \mathcal{S}_i, \mathcal{P}_i^N, E_{elec}^b, r, \hat{N}_{0j}, P_{i,max}^{TX}, \Delta B_i^{(m)}, \hat{Q}_{ij}$

Find : $j^* \in \mathcal{S}_i \cap \mathcal{P}_i^N, P_{ij^*}^{TX*} \leq P_{i,max}^{TX}$

Minimize : $E_i^{(j)} = E_{ij} \cdot \frac{L_P^*}{L_P^* - L_P^H - L_P^F} \cdot \hat{N}_{ij}^{Hop}$ (20)

Subject to :

$$E_{ij}^b = 2 \cdot E_{elec}^b + \frac{P_{ij}^{TX}}{r}; \quad (21)$$

$$L_{P_{ij}}^F = \Psi^{\mathcal{F}^{-1}} \left(L_P^*, PER_{ij}, \Phi^{\mathcal{M}} \left(\frac{P_{ij}^{TX}}{\hat{N}_{0j} \cdot r \cdot TL_{ij}} \right) \right); \quad (22)$$

$$\hat{N}_{ij}^{Hop} = \max \left(\frac{d_{iN}}{< d_{ij} >_{iN}}, 1 \right); \quad (23)$$

$$1 - \left(1 - PER_{ij} \right)^{[\hat{N}_{ij}^{Hop}]} \leq PER_{max}^{e2e}; \quad (24)$$

$$\frac{\tilde{d}_{ij}}{q_{ij}} + \delta \cdot \sigma_{ij}^q \leq \min_{m=1, \dots, M} \left(\frac{\Delta B_i^{(m)}}{\hat{N}_{ij}^{Hop}} \right) - \hat{Q}_{ij} - \frac{L_P^*}{r}. \quad (25)$$

In the following, we explain the extra notations and variables used in the problem formulation for delay-sensitive applications:

- $M = \lfloor (L_T^* - L_T^H) / L_P^* \rfloor$ is the *fixed* number of packets transmitted in a train on each link, where L_T^* and L_P^* are the optimal train length and packet size, respectively, as discussed in Section 4.2.
- PER_{max}^{e2e} and B_{max} [s] are the application-dependent end-to-end packet error rate threshold and delay bound, respectively.
- $\Delta B_i^{(m)} = B_{max} - [t_{i,now}^{(m)} - t_0^{(m)}]$ [s] is the time-to-live of packet m arriving at node i , where $t_{i,now}^{(m)}$ is the arriving time of m at i , and $t_0^{(m)}$ is the time m was generated, which is time-stamped in the packet header by its source.

- $T_{ij} = L_P^* / r + T_{ij}^q$ [s] accounts for the packet transmission delay and the propagation delay associated with link (i, j) , according to Section 3.1; according to measurements on underwater channels reporting symmetric delay distribution of multipath rays [24], we consider a Gaussian distribution for T_{ij} , i.e., $T_{ij} \sim \mathcal{N}(L_P^* / r + \overline{T_{ij}^q}, \sigma_{ij}^q{}^2)$.
- \overline{Q}_i [s] and \overline{Q}_j [s] are the average queueing delays of node i (at the time the node computes its train next hop), and node j , which is a neighbor node of i .
- \hat{Q}_{ij} [s] is the network queueing delay estimated by node i when j is selected as next hop, computed according to the information carried by incoming packets and broadcast by neighboring nodes, as will be detailed in Section 6.1.

The formulation of \mathbf{P}_{sen}^{dist} is quite similar to $\mathbf{P}_{insen}^{dist}$, except for two important differences:

1. The objective function (20) does not include \hat{N}_{ij}^{TX} as in (15), since no selective packet retransmission is performed;
2. Two new constraints are included, (24) and (25), which address the two considered delay-sensitive application requirements, i.e., the end-to-end packet error rate should be lower than an application-dependent threshold PER_{max}^{e2e} , and the probability that the end-to-end packet delay be over a delay bound B_{max} , should be lower than an application-dependent parameter γ , respectively.

Note that (24) adjusts the packet error rate PER_{ij} that will be experienced by packet m on link (i, j) to respect the application end-to-end packet error rate requirement (PER_{max}^{e2e}), given the estimated number of hops to reach the sink if j is selected as next hop (\hat{N}_{ij}^{Hop}). Interestingly, since the packet is assumed to be correctly forwarded up to node i , there is no need to consider the hop count number in (24), i.e., the number of hops of packet m from the source to the current node i . In fact, since node i is assumed to receive the packet, the conditional probability of it being correct is one. Finally, constraint (25) is mathematically derived in the following section. The complexity of \mathbf{P}_{sen}^{dist} is $O(|\mathcal{S}_i \cap \mathcal{P}_i^N|)$, i.e., proportional to the number of its neighboring nodes with positive advance towards the sink.

6.1 Statistical Link Delay Model

In this section, we model the delay of underwater links with the objective of deriving constraint (25) that each link needs to meet in order to statistically limit the end-to-end packet delay. We model the propagation delay of each link (i, j) as a random variable T_{ij}^q , with mean equal to $\overline{T_{ij}^q}$ and variance $\sigma_{ij}^q{}^2$. The mean $\overline{T_{ij}^q} = \tilde{d}_{ij} / q_{ij}$ is computed as the ratio of the average multiple path length \tilde{d}_{ij} and the average underwater propagation speed of an acoustic wave propagating from node i to j (see Section 3.2). In vertical links, sound rays propagate directly without bouncing on the bottom or surface of the ocean. Hence, the multipath effect is negligible, and $\tilde{d}_{ij} \approx d_{ij}$. Conversely, in shallow-water horizontal links, several rays propagate by bouncing on the bottom or surface of the ocean along with the direct ray. Hence, \tilde{d}_{ij} is generally larger than d_{ij} . This is due to the fact that in state-of-the-art underwater receivers, multipath can be compensated for by waiting for the energy associated with delayed rays. This way, it is possible to capture the energy spread on multiple paths, and thus guarantee a smaller BER given a fixed SNR. However, the price for this is that the end-to-end delay may be heavily affected by the propagation delay of several rays.

By leveraging statistical properties of links, we want the probability that a packet exceed its end-to-end delay bound B_{max} to be lower than an application-dependent fixed parameter γ . To achieve this, it should hold that

$$\begin{aligned} \Pr \left\{ [t_{i,now}^{(m)} - t_0^{(m)}] + B_{iN}^{(j)} \geq B_{max} \right\} &= \\ &= \Pr \left\{ B_{iN}^{(j)} \geq \Delta B_i^{(m)} \right\} \leq \gamma, \end{aligned} \quad (26)$$

where $B_{iN}^{(j)}$ is the expected delay a packet will incur from i to the surface station N when j is chosen as next hop, and $\Delta B_i^{(m)} = B_{max} - [t_{i,now}^{(m)} - t_0^{(m)}]$ is the time-to-live of packet m arriving at node i . Node i can estimate the remaining-path delay by projecting, for each possible next hop j , the estimated network queueing delay \hat{Q}_i and the transmission delay T_{ij} to the remaining estimated hops \hat{N}_{ij}^{Hop} , i.e.,

$$B_{iN}^{(j)} \approx (T_{ij} + \hat{Q}_{ij}) \cdot \hat{N}_{ij}^{Hop}, \quad (27)$$

where

$$\hat{Q}_{ij} = \frac{t_{i,now}^{(m)} - t_0^{(m)} - \sum_{(k,h) \in \mathcal{L}_i^{(m)}} \bar{T}_{kh} + \bar{Q}_i + \bar{Q}_j}{N_{HC}^{(m)} + 2}. \quad (28)$$

In (28), the numerator represents the sum of all the queueing delays experienced by packet m in its path $\mathcal{L}_i^{(m)}$, which includes the links from the source generating packet m to node i , and the average queueing delay \bar{Q}_j periodically broadcast by j , while the denominator represents the number of nodes forwarding the packet, including node i , which depends on the hop count $N_{HC}^{(m)}$, i.e., the number of hops of packet m from the source to the current node.

By substituting (27) into (26), and by assuming a Gaussian distribution for T_{ij} , (26) can be rewritten as

$$\begin{aligned} \Pr \left\{ T_{ij} \geq \frac{\Delta B_i^{(m)}}{\hat{N}_{ij}^{Hop}} - \hat{Q}_{ij} \right\} &= \\ &= \frac{1}{2} \left[1 - \operatorname{erf} \left(\frac{\frac{\Delta B_i^{(m)}}{\hat{N}_{ij}^{Hop}} - \hat{Q}_{ij} - \bar{T}_{ij}}{\sqrt{2} \cdot \sigma_{ij}^q} \right) \right] \leq \gamma, \end{aligned} \quad (29)$$

where the erf function is defined as

$$\operatorname{erf}(\Gamma) = \frac{2}{\sqrt{\pi}} \int_0^\Gamma e^{-t^2} dt. \quad (30)$$

Since $\bar{T}_{ij} = L_T^*/r + \bar{T}_{ij}^q$, and $\bar{T}_{ij}^q = \tilde{d}_{ij}/\bar{q}_{ij}$, (29) simplifies to

$$\frac{\tilde{d}_{ij}}{\bar{q}_{ij}} + \delta \cdot \sigma_{ij}^q \leq \frac{\Delta B_i^{(m)}}{\hat{N}_{ij}^{Hop}} - \hat{Q}_{ij} - \frac{L_P^*}{r}, \quad (31)$$

where $\delta = \sqrt{2} \cdot \operatorname{erf}^{-1}(1 - 2\gamma)$ only depends on γ . In particular, δ increases with decreasing values of γ . In addition, in order to consider, as a precautionary guideline, the tightest constraint among all those associated with the M packets to be transmitted in a train, a ‘min’ operator is added, which leads to (25). Note that, while constraint (25) does not bound the delay of a packet, it tries to increase the probability that a packet reach the sink within its delay bound. To achieve this, the proposed algorithm only relies on the past access delay information carried by the packet, and on information about its 1-hop neighborhood, and not on end-to-end signaling. This information is obtained by broadcast messages. However,

Table 1: Simulation Performance Parameters

Parameters	Delay-insensitive	Delay-sensitive
Sensors/average sources	100/100	100/17
Volume	100x100x100 m ³	500x500x50 m ³
Packet size	500 Byte	100 Byte
Packet inter-arrival time	600 s	7.5 s

to limit the overhead caused by these messages, each node advertises its access delay only when it exceeds a pre-defined threshold. Hence, this mechanism allows the routing algorithm to dynamically adapt to the ongoing traffic and the resulting congestion.

7. PERFORMANCE EVALUATION

In this section, we discuss the simulation performance of the proposed routing solutions for delay-insensitive and -sensitive applications, presented in Sections 5 and 6, respectively.

We extended the wireless package of the J-Sim simulator [1], which implements the whole protocol stack of a sensor node, to simulate the characteristics of the underwater environment. In particular, we modeled the underwater transmission loss, the transmission and propagation delays, and the physical layer characteristics of underwater receivers. As far as the MAC layer is concerned, since the development of a new multiple access technique for the underwater environment is out of the scope of this paper and left for future work, we adapted the behavior of the IEEE 802.11 to the underwater environment, although we do not advocate this access scheme for this environment. Firstly, we removed the RTS/CTS handshaking, as it yields unacceptable delays in a low-bandwidth high-delay environment. Secondly, we tuned all the parameters of the IEEE 802.11 according to the physical layer characteristics. For example, the value of the *slot time* in the 802.11 backoff mechanism has to account for the propagation delay at the physical layer [5]. Hence, while it is set to 20 μ s for 802.11 DSSS (Direct Sequence Spread Spectrum), we found that a value of 0.18 s is needed to allow devices a few hundred meters apart to share the underwater medium. This implies that the delay introduced by the backoff contention mechanism is several orders of magnitude higher than in terrestrial channels, which in turn leads to very low channel utilizations. For this reason, we set the values of the contention windows CW_{min} and CW_{max} [5] to 4 and 32, respectively, whereas in 802.11 DSSS they are set to 32 and 1024. We performed two sets of experiments to analyze the performance of the proposed routing solutions. The main parameters differentiating the two sets of experiments are summarized in Table 1.

As far as the delay-insensitive routing algorithm is concerned, we considered 100 sensors randomly deployed in a 3D volume of 100x100x100 m³, which may represent a small harbor. We set the bandwidth to 50 Kbps, the maximum transmission power to 0.5 W, the packet size to 500 Byte, the initial node energy to 1000 J. Moreover, all deployed sensors are source, with packet inter-arrival time equal to 600 s, which allows us to simulate a low-intensity background monitoring traffic from the entire volume. In Fig. 6(a) we show the average node residual energy over the simulation time. In particular, we compare the routing performance when three different link metrics are used. Specifically, the *Full Metric* (15), introduced in Section 5; the *No Channel Estimation*, which does not consider the channel condition, i.e., does not take the expected number of packet transmissions \hat{N}^{TX} into account; and the *Minimum Hops*, which simply minimizes the number of hops to reach the surface station. When the channel state con-

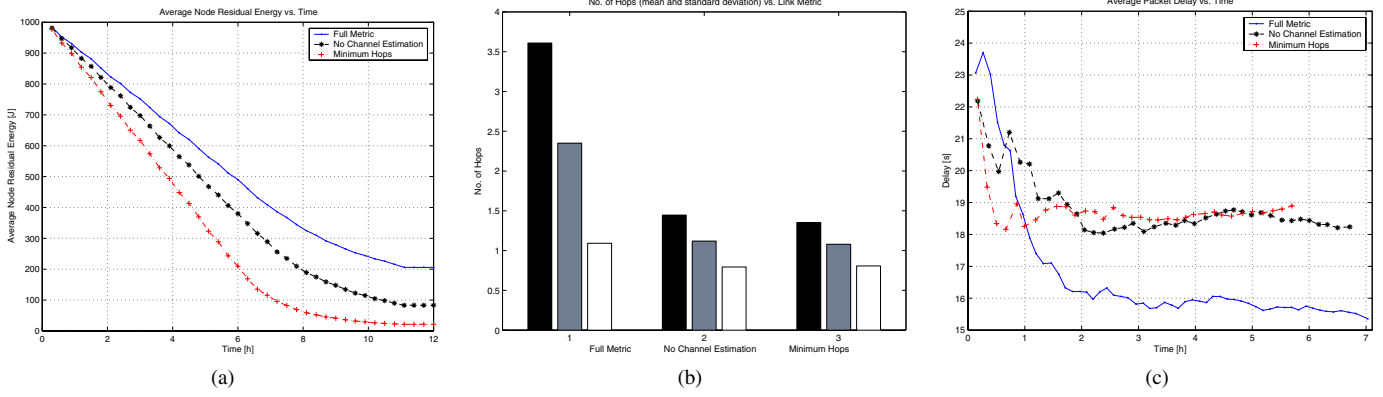


Figure 6: Delay-insensitive routing. (a): Average node residual energy vs. time for different link metrics; (b): Number of hops vs. time; (c): Average packet delay vs. time

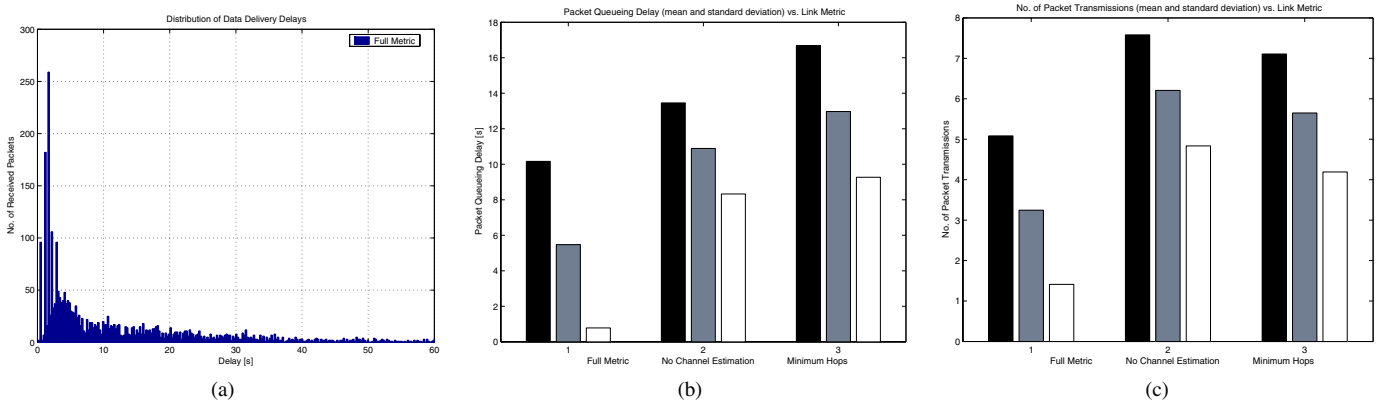


Figure 7: Delay-insensitive routing. (a): Distribution of data delivery delays for the Full Metric; (b): Average node queuing delays with different link metrics; (c): Average number of packet transmissions with different link metrics

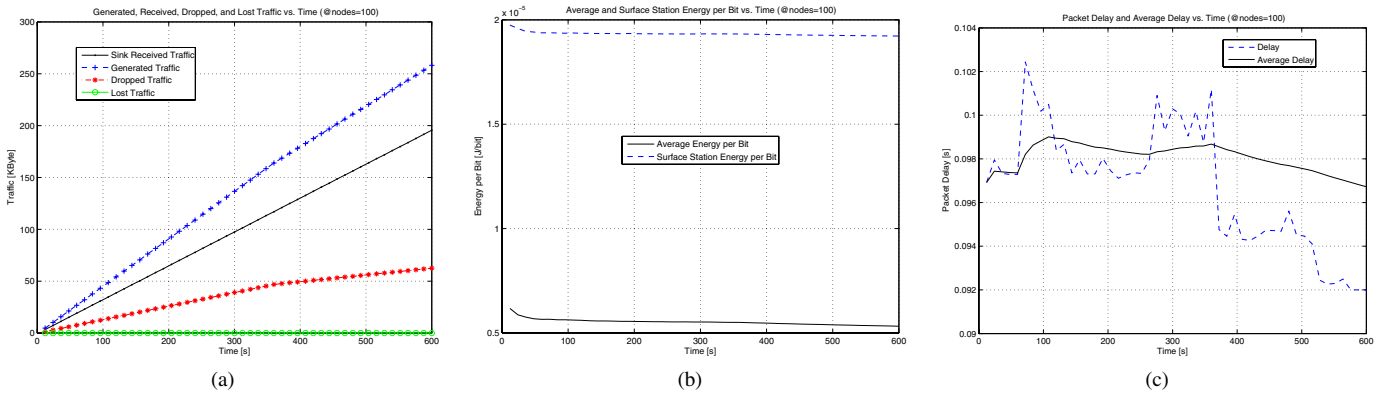


Figure 8: Delay-sensitive routing. (a): Generated, received, dropped, and lost traffic vs. time; (b): Average and surface station used energy per received bit vs. time; (c): Packet delay and average delay vs. time

dition is considered (Full Metric), consistent energy savings can be achieved, thus leading to prolonged network lifetime. In Figs. 6(b) and 6(c), we show the average number of hops and the average packet delays, respectively, when the different link metrics are used. In particular, when the full link metric is adopted, the aver-

age end-to-end packet delays are consistently smaller than with the other metrics, although data paths with the Full Metric are longer, as shown in Fig. 6(b). This is confirmed by Fig. 7(a), where the distribution of data delivery delays is reported for the Full Metric (the delay distributions associated with the other two competing

metrics is omitted for lack of space). This can be explained by the lower average node queuing delays and packet transmissions, depicted in Figs. 7(b) and 7(c), respectively, observed when the full metric is considered. A lower number of packet transmissions (Fig. 7(b)) is in fact to be expected, since the metric explicitly takes the state of the channel into account. Hence, next hops associated to better channels are preferred. This in turn reduces the average queuing delays (Fig. 7(c)) as packets do not necessarily need to be retransmitted.

As far as the delay-sensitive routing algorithm is concerned, Figs. 8(a-c) report its performance when 100 sensors are randomly deployed in a 3D volume of $500 \times 500 \times 50 \text{ m}^3$. Note that, differently from the previous scenario, only some sensors inside an event area of radius 100 m centered inside the monitoring volume are sources of data packets with size 100 Byte and inter-arrival time equal to 7.5 s. In this simulation scenario, we incorporated the effect of the fast fading Rayleigh channel (coherence time set to 0.5 s), to capture the heavy multipath environment in shallow water. Specifically, Fig. 8(a) reports the generated, received, dropped (due to queue overflows), and lost traffic (due to sensor failures), while Fig. 8(b) shows the time evolution of the energy per received bit used by the surface station and by an average node. Figure 8(c) depicts delay and average delay of packets reaching the surface station.

8. CONCLUSIONS

In this paper, the problem of data gathering in a 3D underwater sensor network was investigated, by considering the interactions between the routing functions and the characteristics of the underwater acoustic channel. A model characterizing the acoustic channel utilization efficiency was developed to investigate fundamental characteristics of the underwater environment, and to set the optimal packet size for underwater communications given the application requirements. Two distributed routing algorithms were also introduced, for delay-insensitive and delay-sensitive applications, respectively, with the objective of minimizing the energy consumption taking the varying condition of the underwater channel and the different application requirements into account. The proposed routing solutions were shown to achieve the performance targets of the underwater environment by means of simulation.

Acknowledgments

This work was supported by the Office of Naval Research under contract N00014-02-1-0564.

9. REFERENCES

- [1] The J-Sim Simulator, <http://www.j-sim.org/>.
- [2] M. Abolhasan, T. Wysocki, and E. Dutkiewicz. A Review of Routing Protocols for Mobile Ad Hoc Networks. *Ad Hoc Networks (Elsevier)*, 2:1–22, Jan. 2004.
- [3] K. Akkaya and M. Younis. A Survey on Routing Protocols for Wireless Sensor Networks. *Ad Hoc Networks (Elsevier)*, 3(3):325–349, May 2005.
- [4] I. F. Akyildiz, D. Pompili, and T. Melodia. Underwater Acoustic Sensor Networks: Research Challenges. *Ad Hoc Networks (Elsevier)*, 3(3):257–279, May 2005.
- [5] G. Bianchi. Performance Analysis of the IEEE 802.11 DCF. *IEEE Journal of Selected Areas in Communications*, 18(3):535–547, Mar. 2000.
- [6] P. Bose, P. Morin, I. Stojmenovic, and J. Urrutia. Routing with Guaranteed Delivery in Ad Hoc Wireless Networks. *ACM Wireless Networks*, 7(6):609–616, Nov. 2001.
- [7] D. Codiga, J. Rice, and P. Baxley. Networked Acoustic Modems for Real-Time Data Delivery from Distributed Subsurface Instruments in the Coastal Ocean: Initial System Development and Performance. *Journal of Atmospheric and Oceanic Technology*, 21(2):331–346, 2004.
- [8] F. Fisher and V. Simmons. Sound Absorption in Sea Water. *Journal of Acoustical Society of America*, 62(3):558–564, Sept. 1977.
- [9] S. A. Glegg, R. Pirie, and A. LaVigne. A Study of Ambient Noise in Shallow Water. In *Florida Atlantic University Technical Report*, 2000.
- [10] P. Jacquet, P. Muhlethaler, T. Clausen, A. Laouiti, A. Qayyum, and L. Viennot. Optimized Link State Routing Protocol for Ad Hoc Networks. In *Proc. of IEEE INMIC*, pages 62–68, Pakistan, Dec. 2001.
- [11] D. B. Johnson, D. A. Maltz, and J. Broch. DSR: The Dynamic Source Routing Protocol for Multi-Hop Wireless Ad Hoc Networks. In C. E. Perkins, editor, *Ad Hoc Networking*, pages 139–172. Addison-Wesley, 2001.
- [12] R. Jurdak, C. Lopes, and P. Baldi. Battery Lifetime Estimation and Optimization for Underwater Sensor Networks. *IEEE Sensor Network Operations*, Winter 2004.
- [13] B. Karp and H. Kung. GPSR: Greedy Perimeter Stateless Routing for Wireless Networks. In *Proc. of ACM/IEEE MOBICOM*, pages 243–254, Boston, MA, USA, Aug. 2000.
- [14] T. Melodia, D. Pompili, and I. F. Akyildiz. On the interdependence of Distributed Topology Control and Geographical Routing in Ad Hoc and Sensor Networks. *Journal of Selected Areas in Communications*, 23(3):520–532, Mar. 2005.
- [15] L. Miller. Distribution of Link Distances in a Wireless Network. *Journal of Research of the National Institute of Standards and Technology*, 106(2):401–412, Mar./Apr. 2001.
- [16] D. Moore, J. Leonard, D. Rus, and S. Teller. Robust Distributed Network Localization with Noisy Range Measurements. In *Proc. of ACM SenSys*, Baltimore, MD, USA, Nov. 2004.
- [17] C. Perkins, E. Belding-Royer, and S. Das. Ad Hoc On Demand Distance Vector (AODV) Routing. IETF RFC 3561.
- [18] C. Perkins and P. Bhagwat. Highly Dynamic Destination Sequenced Distance Vector Routing (DSDV) for Mobile Computers. In *Proc. of ACM SIGCOMM*, London, UK, 1994.
- [19] D. Pompili, T. Melodia, and I. F. Akyildiz. A Resilient Routing Algorithm for Long-term applications in Underwater Sensor Networks. In *Proc. of MedHocNet*, Lipari, Italy, June 2006.
- [20] J. Proakis. *Digital Communications*. McGraw-Hill, New York, 1995.
- [21] J. Proakis, E. Sozer, J. Rice, and M. Stojanovic. Shallow Water Acoustic Networks. *IEEE Communications Magazine*, pages 114–119, Nov. 2001.
- [22] V. Ravelomanana. Extremal Properties of Three-dimensional Sensor Networks with Applications. *IEEE Transactions on Mobile Computing*, 3(3):246–257, July/Sept. 2004.
- [23] E. Sozer, M. Stojanovic, and J. Proakis. Underwater Acoustic Networks. *IEEE Journal of Oceanic Engineering*, 25(1):72–83, Jan. 2000.
- [24] M. Stojanovic. Acoustic (underwater) Communications. In J. G. Proakis, editor, *Encyclopedia of Telecommunications*. John Wiley and Sons, 2003.
- [25] M. Stojanovic. Optimization of a Data Link Protocol for an Underwater Acoustic Channel. In *Proc. IEEE OCEANS*, Brest, France, June 2005.
- [26] I. Stojmenovic. Localized Network Layer Protocols in Wireless Sensor Networks Based on Optimizing Cost over Progress Ratio. *IEEE Networks*, 20(1):21–27, Jan./Feb. 2006.
- [27] R. J. Urlick. *Principles of Underwater Sound*. McGraw-Hill, 1983.
- [28] I. Vasilescu, K. Kotay, D. Rus, M. Dunbabin, and P. Corke. Data Collection, Storage, and Retrieval with an Underwater Sensor Network. In *Proc. of ACM SenSys*, San Diego, CA, USA, Nov. 2005.
- [29] G. Xie and J. Gibson. A Network Layer Protocol for UANs to Address Propagation Delay Induced Performance Limitations. In *Proc. of IEEE OCEANS*, volume 4, pages 2087–2094, Honolulu, HI, Nov. 2001.
- [30] P. Xie, J.-H. Cui, and L. Lao. VBF: Vector-Based Forwarding Protocol for Underwater Sensor Networks. In *Networking*, pages 1216–1221, Coimbra, Portugal, May 2006.